

ents			n						
API X 52	0. 12	1. 22	0. 23	0.0 01	0.0 11	0.0 3	0. 03	0.0 02	0.0 34

Fracture surfaces of Charpy impact specimens were analyzed using a JEOL JSM-6360LV Scanning electron microscope.

To obtain dual phase steels with various morphologies, three kinds of heat treatment were used as shown in Fig.1. Specimens were cut from different treatments and mounted for metallographic examination. Standard grinding and polishing techniques were employed, and specimens were etched with 3 pctnital solution. Conventional light microscopy was used to make a comparative examination of the overall microstructure of the API X52 steel. Tensile testing was conducted at room temperature in a computer controlled Mohr FederhaffLasenhausen System Machine. According to ASTM A370, standard specimen for Charpy impact tests were

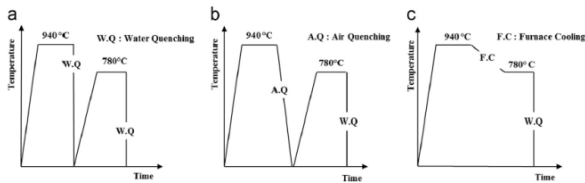


Figure 1. Schematic representation of heat treatments schedules for (a) IQ-W (b) IQ-A (c) SQ treatments.

3 RESULTS AND DISCUSSION

3.1 Microstructures

Fig. 2 shows the optical micrographs of API X52 (DP) steel subjected to different heat treatment schedules treated at Intercritical Annealing Temperature (IAT) =780°C. The IQ/W microstructures showed fine and fibrous martensite uniformly distributed within the ferrite matrix (Fig. 2a), whereas IQ/A microstructure showed polygonal ferrite surrounded by martensite network (Fig. 2b) and SQ microstructures revealed blocky and banded ferrite–martensite phase (Fig. 2c). The difference in the microstructural state of the specimen reached before intercritical treatment may be held responsible for the observed differences in the martensite morphologies and distributions. In IQ/W treatment, martensitic microstructures were annealed in the (α+γ) region which provides numerous sites for nucleation of both the austenite

and ferrite phases. The nucleation of austenite from the initial martensitic microstructure starts at the prior austenite grain boundaries, and also at the martensite lath boundaries. The microstructures developed with prior pearlite-ferrite phases (IQ/A treatment) consisted of polygonal ferrite surrounded by dark etching martensite network, especially along the ferrite/ferrite grain boundaries, following the location of pearlite in the initial (ferrite+pearlite) microstructure. In the case of SQ treatment

, the initial phase before two phases annealing is austenite. Upon decreasing the temperature to the (α+γ) region, ferrite nucleates at the grain boundaries of austenite and grows within the austenite grains [6,7]. Such a ferrite–austenite structure has resulted into a (DP) microstructure with alternate bands of ferrite and martensite after quenching from (α+γ) region. The martensite volume fractions (MVF) obtained under (IQ), (DQ) and (SQ) treatments were quantified at 52 %, for the annealing temperatures of 760 °C. Similar IAT of 780 °C resulted in identical martensite content for different intercritical heat treatments was reported by Ahmed et al. [7]

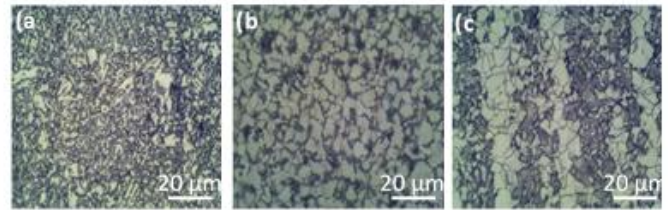


Figure 2: Optical micrographs of a) IQ/W, b) IQ/A, and c) SQ treatments, showing ferrite (white) and martensite (black).

3.2 Mechanical properties.

The yield, ultimate tensile strength and elongation of IQ/A, IQ/W and SQ treatments are shown in Table 2. The tensile properties change significantly with the heat treatment schedules, which can be attributed to the difference of ferrite-martensite morphologies, and distributions. The highest yield strength (500 MPa) and ultimate tensile strength (800 MPa) was observed with the IQ/water microstructure. Among the different treatments, IQ/W treatment clearly yields the most attractive combination of strength and ductility compared to IQ/A and SQ treatments. The lowest elongation of SQ treatment is probably due to the fact that

ferrite grains fracture in a brittle mode prior to the martensite fracture during necking. This is caused by the local internal stress produced in the vicinity of the ferrite/martensite interface during deformation [7]. In the IQ/W specimen (Fig. 2a), finer and fibrous martensites restrict the growth of microvoids as they encounter the frequent discontinuities in the ferrite/martensite interfaces which delay the void coalescence resulting into higher values of elongation to failure. However, in the case of IQ/Air microstructure (Fig. 2b), the microvoids formed at the ferrite/martensite interfaces can easily grow along the grain boundaries continuously due to the fact such grain boundaries are having higher concentration of transformation strain and are nearly continuous.

Table 2. Tensile and Charpy impact properties of X52 DP steels treated at 780°C.

	YS(MPa)	UTS (MPa)	A (%)	USE (J)	DBTT (°C)
IQ/W	500	800	28	210	< - 60
IQ/A	452	700	19	154	- 50
SQ	485	720	12	23	- 12

3.3 Charpy Impact and fracture properties

In HSLA steels, strength is mainly represented by yield strength, while toughness is largely considered in terms of (DBTT) and absorption energy at a given temperature or upper-shelf energy USE. The variation of Charpy impact energy test data from specimens annealed at 780°C under IQ/A, IQ/W and SQ treatments, as a function of test temperatures are shown in Fig. 3. The data indicate that the DBTT of the IQ/W specimen based on the criterion of 28 J absorbed energy is lower than - 60 °C. The DBTT of the SQ and the IQ/A specimens are -12°C and -50°C, respectively. The USE values of the IQ/A treatment begins at approximately 0°C with absorbed energy of about 154 J, and the USE of the SQ treatment begins at approximately +20°C with absorbed energy of about 100 J. The DBTT of the SQ treatment is higher than that of the IQ/W treatment because the SQ microstructure contains a considerable amount of continuous coarse ferrite and martensite with probably large effective grain size. Hence, it can be concluded that higher toughness values in IQ/W specimens are associated with finer martensite. It is interesting to note that the Charpy impact energy value tested at room temperature is higher for IQ/W treatment than for IQ/A treatment and SQ treatment at comparable Vm.

This substantiates the fact that the finely dispersed ferrite is beneficial to toughness [2]. The fracture surfaces of IQ/W, IQ/A and SQ specimens tested at room temperature are presented in Fig. 4.

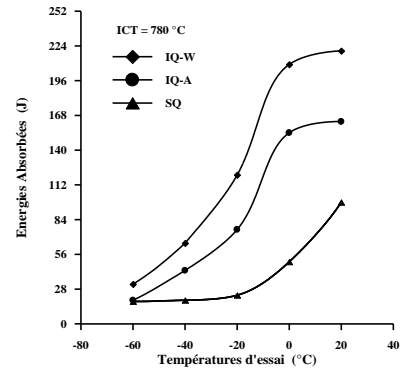


Figure 3. Charpy impact energy as a function of temperature of all treatment treated at 780°C

first or by ferrite–martensite interfacial separation [8]. Micro-cracks propagate either by cleavage or by dimple mode, depending on the state of the stress present in the microstructures.

It reveals mixtures of cleavage and dimples for all the specimens. The area of cleavage surfaces increases in the order of SQ > IQ/A > IQ/W treatments, whereas the areas of dimples increase in the reverse order. The size of dimple in the IQ/W treatment is extremely fine compared to the SQ specimen, indicating higher impact energy value tested at + 20 °C for the IQ/W (210 J) than the SQ (99 J). This is probably due to the presence of large blocky martensite zone. The fracture surfaces of IQ/W, IQ/A and SQ specimens tested at -40 °C are presented in Fig. 5. The SQ specimen shows a completely brittle cleavage cracking, and complex river patterns consisting of small cleavage steps (Fig. 5c) while in the IQ/W specimen, both dimples and cleavage facets can be seen. When load is applied to (FMDP) steels, it is anticipated that fracture occurs by fracture of hard martensite

(a)

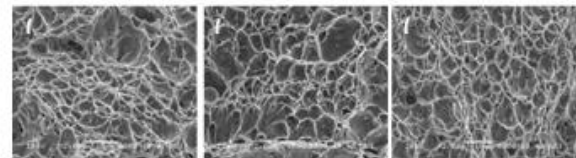


Figure 4. SEM Fractographs of Charpy impact specimens fractured at R.T., a) IQ/A, b) IQ/W, c) SQ

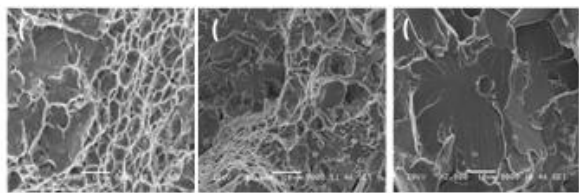


Figure 5. SEM Fractographs of Charpy impact of specimens fractured at $-40\text{ }^{\circ}\text{C}$, a) IQ/A, b) IQ/W and c) SQ

4 CONCLUSIONS

On the basis of the experimental work that has been carried out and presented in this article, the following conclusions can be drawn.

1. Prior microstructure has a great influence on the evolution of ferrite and martensite morphologies.
2. IQ/W, IQ/Air and SQ treatments resulted in fine and fibrous martensite uniformly distributed within the ferrite, polygonal ferrite surrounded by martensite network and blocky and banded ferrite-martensite microstructures, respectively.
3. IQ/W treatment provided the best combination of strength and ductility of DP steels with fine and fibrous martensite morphologies.
4. IQ/W treatment exhibited better impact properties than IQ/Air and SQ treatments as expressed by its lower DBTT and higher USE values.

REFERENCES

- [1] R.O. Rocha, T.M.F. Melo, E.V. Pereloma, D.B. Santos, Microstructural evolution at the initial stages of continuous annealing cold rolled dual phase steel, *Materials Science and Engineering: A*, 391 (2005) 296-304. [DOI:10.1016/j.msea.2004.08.081](https://doi.org/10.1016/j.msea.2004.08.081).
- [2] M. Nishiyama, K. Park, N. Nakada, T. Tsuchiyama, Effect of the martensite distribution on the strain hardening and ductile fracture behaviors in dual-phase steel, *Materials Science and Engineering: A*, 604 (2014) 135-141. [DOI:10.1016/j.msea.2014.02.058](https://doi.org/10.1016/j.msea.2014.02.058).
- [3] A. Bag, K.K Ray, E.S. Dwarakadasa, Influence of martensite content and morphology on tensile and impact properties of high-martensite dual-phase steels, *Metallurgical Transaction A* 30 (1999) 1193–1202. [DOI:10.1007/s11661-999-0269-4](https://doi.org/10.1007/s11661-999-0269-4).
- [4] H. Seyedrezai, A.K. Pilkey, J.D. Boyd, Effect of pre-annealing treatments on the final microstructure and work hardening behavior of a dual-phase steel, *Materials Science and Engineering: A*, 594 (2014) 178-188. [DOI:10.1016/j.msea.2013.11.034](https://doi.org/10.1016/j.msea.2013.11.034).
- [5] E. Fereiduni, S.S.G. Banadkouki, Improvement of mechanical properties in a dual-phase ferrite–martensite 4140 steel under tough-strong ferrite formation, *Materials & Design*, 56 (2014) 232-240. [DOI:10.1016/j.matdes.2013.11.005](https://doi.org/10.1016/j.matdes.2013.11.005).
- [6] A. Karmakar, M. Ghosh, D. Chakrabarti, cold-rolling and inter-critical annealing of low-carbon steel: effect of initial microstructure and heating-rate, *Materials Science and Engineering: A564* (2013) 389-399. [DOI:10.1016/J.MSEA.2012.11.109](https://doi.org/10.1016/J.MSEA.2012.11.109).
- [7] E. Ahmed, T. Manzoor, M.M.A. Ziai, N. Hussain, Effect of martensite morphology on tensile deformation of dual-phase steel, *Journal of Materials Engineering and Performance*, 21 (2012) 382-387. [DOI:10.1007/s11665-011-9934-z](https://doi.org/10.1007/s11665-011-9934-z).
- [8] B. Hwang, C.G. Lee, S.J. Kim, Low-temperature toughening mechanism in thermomechanically processed high-strength low-alloy steels, *Metallurgical and Materials Transactions A* 42 (2011) 717–728. [DOI:10.1007/s11661-010-0448-3](https://doi.org/10.1007/s11661-010-0448-3)